



This is a repository copy of *Metabolic Phenotyping of CHO Cells Varying in Cellular Biomass Accumulation and Maintenance during Fed-Batch Culture*.

White Rose Research Online URL for this paper:

<https://eprints.whiterose.ac.uk/123247/>

Version: Accepted Version

Article:

Fernandez-Martell, A., Johari, Y.B. and James, D.C. (2018) Metabolic Phenotyping of CHO Cells Varying in Cellular Biomass Accumulation and Maintenance during Fed-Batch Culture. *Biotechnology and Bioengineering*, 115 (3). pp. 645-660. ISSN 0006-3592

<https://doi.org/10.1002/bit.26485>

This is the peer reviewed version of the following article: Fernandez-Martell A, Johari YB, James DC. Metabolic phenotyping of CHO cells varying in cellular biomass accumulation and maintenance during fed-batch culture. *Biotechnology and Bioengineering*. 2018; 115: 645–660, which has been published in final form at <https://doi.org/10.1002/bit.26485>. This article may be used for non-commercial purposes in accordance with Wiley Terms and Conditions for Use of Self-Archived Versions. This article may not be enhanced, enriched or otherwise transformed into a derivative work, without express permission from Wiley or by statutory rights under applicable legislation. Copyright notices must not be removed, obscured or modified. The article must be linked to Wiley's version of record on Wiley Online Library and any embedding, framing or otherwise making available the article or pages thereof by third parties from platforms, services and websites other than Wiley Online Library must be prohibited.

Reuse

Items deposited in White Rose Research Online are protected by copyright, with all rights reserved unless indicated otherwise. They may be downloaded and/or printed for private study, or other acts as permitted by national copyright laws. The publisher or other rights holders may allow further reproduction and re-use of the full text version. This is indicated by the licence information on the White Rose Research Online record for the item.

Takedown

If you consider content in White Rose Research Online to be in breach of UK law, please notify us by emailing eprints@whiterose.ac.uk including the URL of the record and the reason for the withdrawal request.



eprints@whiterose.ac.uk
<https://eprints.whiterose.ac.uk/>

Cellular and Metabolic Engineering

Biotechnology and Bioengineering
DOI 10.1002/bit.26485

**Metabolic Phenotyping of CHO Cells Varying in Cellular Biomass Accumulation and
Maintenance during Fed-Batch Culture[†]**

Running title: Metabolic phenotyping of CHO cells.

Alejandro Fernandez-Martell, Yusuf B. Johari, David C. James*

Department of Chemical and Biological Engineering, University of Sheffield, Mappin St.,
Sheffield, S1 3JD, U.K.

*to whom correspondence should be addressed.

telephone: +44 (0)114 222 7505

email: d.c.james@sheffield.ac.uk

[†]This article has been accepted for publication and undergone full peer review but has not been through the copyediting, typesetting, pagination and proofreading process, which may lead to differences between this version and the Version of Record. Please cite this article as doi: [10.1002/bit.26485]

This article is protected by copyright. All rights reserved

Received August 13, 2017; Revision Received October 13, 2017; Accepted October 23, 2017

This article is protected by copyright. All rights reserved

ABSTRACT

CHO cell lines capable of high-level recombinant protein product biosynthesis during fed-batch culture are still generally obtained by intensive empirical screening of transfected cells rather than knowledge-guided cellular engineering. In this study, we investigate how CHO cell lines create and maintain cellular biosynthetic capacity during fed-batch culture to achieve the optimal combination of rapid exponential proliferation and extended maintenance of high cell biomass concentration. We perform a comparative meta-analysis of mitochondrial and glycolytic functions of 22 discrete parental CHO cell lineages varying in fed-batch culture performance to test the hypotheses that (i) “biomass-intensive” CHO cells exhibit conserved differences in metabolic programming and (ii) it is possible to isolate parental CHO cell lines with a biomass-intensive phenotype to support fed-batch bioproduction processes. We show that for most parental CHO cell lines, rapid proliferation and high late-stage culture performance are mutually exclusive objectives. However, quantitative dissection of mitochondrial and glycolytic functions revealed that a small proportion of clones utilize a conserved metabolic program that significantly enhances cellular glycolytic and mitochondrial oxidative capacity at the onset of late-stage culture. We reveal the central importance of dynamic metabolic re-programming to activate oxidative mitochondrial function as a necessary mechanism to support CHO cell biosynthetic performance during culture. This article is protected by copyright. All rights reserved

Keywords: Chinese hamster ovary cells, metabolic phenotype, cell biomass, directed evolution, mitochondria, glycolysis.

INTRODUCTION

Industrial procedures to create and isolate high-performance CHO cell lines for biopharmaceutical manufacturing process development are currently reliant upon high-throughput screening technologies to identify clonal isolates with favorable cell culture process performance (i.e. production, stability) and recombinant product attributes. Although previous studies have identified alterations in CHO metabolism associated with transition through cell culture phases (Ahn and Antoniewicz 2011; Ahn and Antoniewicz 2013; Templeton et al. 2013; Young 2013), we still do not generally understand how some CHO cells, and not the majority of others, can adapt metabolic function to achieve both rapid proliferation and maintenance of high viable cell biomass *in vitro*.

Substantial increases in cellular biomass synthesis *in vitro* have been obtained over recent years, typically as a result of iterative empirical media, feed and process design rather than *a priori* knowledge-guided genetic engineering of cellular controls on biomass synthesis. Despite efforts to engineer CHO cell metabolism by a variety of means (Dorai et al. 2009; Wilkens and Gerdtzen 2011; Wlaschin and Hu 2007; Zhou et al. 2011), cells in chemically-defined media generally still proliferate slowly (doubling time 20–24h) and the specific rate of biomass synthesis markedly declines during culture. Screening of engineered CHO cell populations with varying genetic/functional properties is generally the route taken to obtain clonal derivatives with improved bioproduction capability (Porter 2015; Prentice et al. 2007; Sinacore et al. 2000). Related to this, deliberate mining of the functional (phenotypic) diversity of host cell clones offers the opportunity to isolate efficient, but rare, clonal variants with enhanced biomanufacturing capabilities (Davies et al. 2012; O'Callaghan et al. 2015). However, to the best of our knowledge, no studies have analyzed, from a metabolic programming perspective, how maximal rates of CHO cell biomass synthesis are achieved by some clones and not others. In this study we functionally dissect the cellular bioenergetics,

specifically mitochondrial and glycolytic functions of 22 discrete CHO clonal lineages varying in the extent to which they can create and maintain cell biomass during fed-batch culture. We reveal that high-performance “biomass-intensive” parental CHO cells employ a rare but conserved metabolic phenotype characterized by an ability to switch-on oxidative metabolism at the onset of stationary-phase culture. We show that it is possible to obtain significantly improved host CHO cell phenotypes by analysis of multi-parallel subcultures, exploiting acquired diversity in metabolic programming.

MATERIALS AND METHODS

CHO-S cell cloning and long-term cell culture

A donor parental CHO-S cell line (Life Technologies, Paisley, UK) was used to isolate 22 clonally-derived cell lines using two rounds of limited dilution cloning (LDC) in 96-well plates as described previously (Davies et al. 2012), yielding a probability of clonality of 0.97 and a cloning efficiency of 1.15%. After 63 days of expansion in static culture in CD-CHO medium containing 8 mM L-glutamine – with a sequential scaling up from 96-well plate into a 24-well plate, 6-well plate, and T-75 cell culture flask, 22 clonally-derived cell lines were transferred into individual 125 mL Erlenmeyer suspension culture flasks, maintained at 37°C, 140 rpm under 5% CO₂ and cultured until cell viability was recovered and maintained above 95% for three consecutive passages. At this point, generation number was set at zero and cells were sampled for cell banking.

For extended exponential subculture up to 220 generations, clonally-derived cell lines were routinely maintained in TubeSpin bioreactor tubes (TPP, Trasadingen, Switzerland) at a working volume of 6 mL in glutamine-supplemented (8 mM) CD-CHO medium at 37°C, 140 rpm under 5% CO₂. Cells were subcultured every 3–4 days at a seeding density of 2×10^5 viable cells mL⁻¹. Cell density and viability were routinely measured using the Vi-CELL XR

(Beckman Coulter, High Wycombe, UK) and cell samples (subclones) were cryopreserved at approximately 80 and 200 generations. Cell specific growth rate (μ) and generation number (GN) were calculated as previously described (Davies et al., 2013).

Prior to cryopreservation, cells were harvested at mid-exponential growth phase, centrifuged at 200 \times g for 5 min and resuspended in cold glutamine-supplemented CD-CHO medium containing 10% (v/v) DMSO at a density of 6.6 \times 10⁶ viable cells mL⁻¹. Aliquots (1.5 mL) were dispensed into cryovials (Thermo Scientific Nunc, Loughborough, UK) and placed immediately into a controlled-rate freezing container (Thermo Scientific Nunc). Cryovials were placed in a -20°C freezer for 4 h, transferred into a -80°C freezer overnight and then into a liquid nitrogen cryostat for long-term storage.

Fed-batch culture of CHO-S subclones

A multi-day supplementation strategy was optimized using CD-CHO EfficientFeed B (Life Technologies) as nutrient supplement according to the manufacturer's instructions. The feeding strategy supporting the highest peak viable cell concentration (VCC) and integral of viable cell concentration (IVCC) performance was selected as the optimal feeding regimen. Optimized fed-batch culture (FBC) performance was carried out after four passages post-thaw. Briefly, FBCs were inoculated at 2 \times 10⁵ viable cells mL⁻¹ in 125 mL Erlenmeyer shake flasks containing 25 mL of glutamine supplemented CD-CHO medium. The multi-day supplementation regime consisted in adding 10% (v/v) CD-CHO EfficientFeed B at days 3, 5, 7 and 9. VCD, cell viability and cell diameter were assessed daily using the Vi-CELL XR. All cultures were maintained at 37°C, 140 rpm under 5% CO₂ until cell viability dropped below 60%. Across all cell populations analyzed, a Gaussian frequency distribution of cell diameter/volume was evident. Therefore, we confidently utilized mean cell volume as a reliable

population descriptor. The IVCC and integral of viable cell volume (IVCV) were calculated as follows:

$$\text{IVCC} [\text{cell h mL}^{-1}] = \frac{(X_1 - X_0)(t_1 - t_0)}{\text{Ln}\left(\frac{X_1}{X_0}\right)} \quad (\text{Equation 1}) \quad (\text{Prentice et al. 2007})$$

$$\text{IVCV} [\text{mm}^3 \text{ h mL}^{-1}] = \frac{(V_1 X_1 - V_0 X_0)(t_1 - t_0)}{\text{Ln}\left(\frac{X_1}{X_0}\right)} \quad (\text{Equation 2})$$

where X_1 and X_0 are the VCC at final and initial time points, respectively, t_1 and t_0 are the time at final and initial time points, respectively, V_1 and V_0 are the mean cell volume at final and initial time points, respectively.

Mitochondrial and glycolytic extracellular flux bioenergetics analysis

Oxygen consumption rate (OCR) and extracellular acidification rate (ECAR) were measured using the cell metabolic analyzer Seahorse XF24 (Seahorse Biosciences, North Billerica, MA) according to the manufacturer's instructions. Briefly, 1.2×10^6 viable cells well^{-1} were plated in Seahorse XF24 plates previously coated with BD Cell-Tak cell and tissue adhesive (BD Biosciences, Oxford, UK; $22.4 \mu\text{g mL}^{-1}$ for 20 min) and incubated at 37°C under 5% CO_2 in a static incubator for 30 min. Conditioned media was replaced with 600 μL of unbuffered Seahorse XF media, supplemented with 2 mM L-glutamine and 16.74 mM glucose (pH 7.4) for the OCR analysis or with only 2 mM L-glutamine for the ECAR analysis. Plates were immediately incubated at 37°C in a CO_2 -free incubator for 30 min before being loaded onto the analyzer. Three real-time measurements of OCR and ECAR were directly measured (basal readings) and after injection of different mitochondrial inhibitors or glycolytic modulators. For OCR, the cells were sequentially treated with optimized concentrations of oligomycin (1 μM), carbonyl cyanide p-[trifluoro-methoxy]-phenyl-hydrazone (FCCP; 1.25 μM) and rotenone/antimycin A (1 μM), while for ECAR the cells were sequentially treated with optimized concentration of glucose (10 mM), oligomycin (1.125 μM) and 2-deoxy-D-glucose

(100 mM). Cell seeding, oligomycin, FCCP, rotenone and antimycin A concentrations were optimized according to the manufacturer's instructions. To exclude any cell volume effects across clonal derived cell lines, all specific metabolic rates, mitochondrial and glycolytic activities were corrected for cell volume using the following volume factor:

$$\text{Volume factor} = \frac{V_{\text{cell}}}{\frac{\sum_i^n V_{\text{cell}}}{n}} \quad (\text{Equation 3})$$

where V_{cell} is the mean cell volume of each individual cell line in the study, n is the total number of cell lines in the study.

Metabolite assay

Prior to analysis, culture medium was centrifuged at 200×g for 5 min to remove cells. Glucose, lactate and glutamine concentrations were determined by colorimetric methods using the Cedex Bio (Roche Diagnostics, West Sussex, UK) according to the manufacturer's instructions. The specific metabolic flux rate (qMet) was calculated as follows:

$$\text{qMet [pmol cell}^{-1} \text{ h}^{-1}] = \frac{Met_1 - Met_0}{IVCC_1 - IVCC_0} \quad (\text{Equation 4})$$

where Met_1 and Met_0 are the final and initial metabolite concentrations, respectively, $IVCC_1$ and $IVCC_0$ are the IVCC at final and initial time points, respectively.

Transient fed-batch production of recombinant proteins

Plasmids encoding recombinant secreted alkaline phosphatase (SEAP) and Sp35Fc fusion proteins were transfected into CHO-S subclones by lipofection, then cultured by FBC for 10 days (as described above), and the recombinant protein product concentration assayed in cell-free supernatant as previously described (Johari et al. 2015).

RESULTS

CHO subclone proliferation, biomass synthesis and fed-batch culture performance

We initially investigated whether subclonal variation in cell specific μ was related to variation in FBC performance. We hypothesized that increased exponential growth rate would be inversely proportional to late stage culture performance as CHO cell metabolism during rapid exponential growth is dominated by Warburg-type aerobic glycolysis (Ahn and Antoniewicz 2013; Templeton et al. 2013; Young 2013), and increasing adaptation to this metabolic program to support rapid proliferation would require a proportionately large shift back to oxidative metabolism to support late stage culture performance.

Each clonally-derived cell line was routinely sub-cultured using a 3-4 day split regime for more than 200 generations. As shown in Fig. 1, after an initial adaptation phase of approximately 50 generations, the mean specific growth rate increased linearly between generations 50 and 200, from 0.033 ± 0.003 to 0.040 ± 0.003 h^{-1} with an overall average rate of change in μ ($\Delta\mu$) of 2.99×10^{-5} h^{-1} generation $^{-1}$ (Fig. 1, inset).

Cell samples from all 22 clonal isolates were removed from cryopreservation at 0, 80 and 200 generations representing early, mid and maximally evolved phases respectively, and FBC performance was measured after four passages post-thaw. Substantial subclone specific variation in culture performance with respect to viable cell concentration (VCC; Fig. 2A) and the integral of viable cell concentration (IVCC; Fig. 2B) were evident. As expected, the maximally evolved (200 generation) subclonal populations generally exhibited a significantly higher cumulative IVCC during the first 7 days of culture (Fig. 2C) although their subsequent cumulative IVCCs (post-day 7) were generally significantly below that of clonal subpopulations evolved for shorter periods (Fig. 2D). Despite this general trend, a substantial clone-specific variation was maintained. For example, across all subclones the total IVCC over FBC varied 3-fold (from 1417 to 4207×10^6 cell h mL^{-1}) and exponential μ varied 1.4-fold (from

0.030 to 0.041 h⁻¹; Fig. 2E). Across all subclones, we found that increased growth rate was inversely correlated with cell volume (PPMCC $r = -0.56$, p-value < 0.001, Fig. 2E). Since it has been observed that CHO (and other transformed mammalian) cell biomass is directly proportional to cell volume (Davies et al. 2012; Dolfi et al. 2013; Frame and Hu 1990), we utilized both clone-specific daily VCC and cell volume measurements over the course of FBC (cell volume tending to decline as culture progressed; data not shown) to calculate the integral of viable cell mean volume (IVCV) over FBC as a simple indirect measurement of total cell biomass synthesis. This is analogous to measurement of packed cell volume (Stettler et al. 2006). These data revealed that IVCV positively correlated with exponential phase μ (PPMCC $r = 0.67$, p-value < 0.001, not shown). Even though cells evolved for 200 generations were generally smaller (Fig. 2E), they were capable of higher relative biomass accumulation (IVCC and IVCV) during exponential phase growth, which supported generally similar IVCV performance over FBC (Fig. 2F). However, for the majority of subclones late stage culture performance was inversely proportional to increased exponential growth rates (Fig. 2C, D). Only 3/22 clones evolved for 200 generations (2, 4, and 17) maintained both high IVCC and IVCV during late stage culture. Our data reveal that for these unusual subclones, improved late stage FBC performance was either actually acquired during progressive subculture (subclones 2, 17; Fig. 2D) or was stably maintained throughout (subclone 4). Other clones evolved for shorter periods (e.g. subclones 1, 11 at 80 generations) also exhibited relatively high late stage culture performance, although this was not subsequently maintained over extended subculture. Taken together, these data reveal that (i) the media/growth environment did not limit biomass accumulation during FBC for the majority of clones *per se*, (ii) generally, but not exclusively, exponential growth rate is inversely proportional to late stage culture performance, (iii) for a small proportion of subclones late stage culture performance can be considered a neutral trait with respect to the selective pressure (exponential growth rate) and is subject to variable genetic

drift and (iv) only a minor proportion of subclones exhibit functional stability (proliferation, FBC performance) over extended subculture.

Optimal fed-batch culture performance is associated with elevated cellular mitochondrial and glycolytic capacities acquired at the onset of stationary phase culture

In order to compare the relative ability of subclones sampled at varying stages of evolutionary subculture to create and maintain cellular biomass during FBC we plotted IVCC against IVCV.

We assumed that subclones exhibiting optimal FBC performance maximize both the number of cellular genomes synthesized (IVCC) and the cellular biomass surrounding these genomes (IVCV). In the hypothetical context of a stably transfected CHO cell, this would maximize both the number of recombinant gene copies and cellular biomass capacity available to synthesize the recombinant protein product. These data, shown in Fig. 3A, reveal substantial (almost 4-fold) variation in FBC performance, where IVCC and IVCV are linearly related, which was expected as these derivative integrals are not independent. The majority of subclones exhibiting optimal performance according to these criteria were those that were maintained in subculture for 80 or 200 generations and had acquired strong late stage culture performance against the general evolutionary trend as previously described (identified as *subclone.generation* in subculture: 1.80, 11.80, 2.200, 4.200, 17.200). This minority of subclonal populations (5/66) were clearly distinct. For subsequent comparative analyses of metabolic function (below) we sampled three clusters of subclonal populations interspaced across the linear axis relating IVCC and IVCV representative of low (5 subclonal populations), mid (9 subclonal populations) and high (5 subclonal populations) FBC performance (indicated in Fig. 3A). Analysis of these groups with respect to IVCC during culture showed that although higher performing subclones were generally capable of more rapid exponential proliferation

(Fig. 3B) the majority of variation in FBC performance was a consequence of clear differences in the accumulation and maintenance of cell numbers during late stage culture (Fig. 3C).

To determine whether the subclonal populations varying in FBC performance (low, mid, high; Fig. 3A) exhibited conserved differences in their utilization of major carbon and nitrogen sources (glucose, lactate, and glutamine), the cell specific flux of each metabolite was measured at days 3 and 7 post-inoculation, representing exponential and (onset) stationary phases of FBC respectively. Differences in metabolite flux normalized with respect to cell volume were compared (Fig. 4). These data revealed no significant heterogeneity in exponential phase glucose consumption and lactate production (Fig. 4A, B), where the majority of subclones exhibited Lac:Glu flux ratios >2 (not shown), indicating the utilization of medium components (e.g. amino acids) other than glucose to generate lactate. It is well known that rapidly proliferating cancer cells actively metabolize glutamine and other amino acids to pyruvate (via malic enzyme) to generate NADPH (DeBerardinis et al. 2007; Vander Heiden et al. 2009). However, there was a clear trend towards increased exponential phase glutamine consumption associated with elevated exponential growth and FBC performance (Fig. 4C). Across all subclonal populations stationary phase consumption of glutamine was nil (as this was not supplied in feeds), with no evidence of lactate resorption. However, glucose consumption continued (supplied in feeds), although at a relatively reduced rate ($<23.4\%$) in cells exhibiting high FBC performance (Fig. 4A).

We hypothesized that the relative ability of cells to both proliferate rapidly and/or to achieve high late stage culture performance would require conserved variation in mitochondrial functions as this organelle is central to both biosynthetic precursor generation to support rapid proliferation and increased oxidative metabolism during late stage culture (Templeton et al. 2013; Young 2013) – see also Pires das Neves et al. (2010). Accordingly, we utilized microplate-based measurement of oxygen consumption by live cells (Seahorse Bioscience XF

Analyzer) to compare the mitochondrial function of subclones at both exponential (Day 3) and stationary (Day 7) phases of culture. This platform technology also permits comparative analysis of glycolytic function by measurement of ECAR (Divakaruni et al. 2013; TeSlaa and Teitell 2014). These data are shown in Fig. 5 and Fig. 6. To facilitate comparative analysis we show mitochondrial and glycolytic functions of subclones clustered into low, medium and high performance rate groups as described previously (Fig. 3A).

For each clonal derivative mitochondrial functions (basal respiration, ATP turnover, proton leak, maximal respiration, spare respiratory capacity, coupling efficiency and non-mitochondrial respiration) were determined according to Brand and Nicholls (2011) by combining the sequential effects of optimized concentrations of oligomycin (ATP synthase inhibitor), FCCP (electron transport chain accelerator) and rotenone plus antimycin A (ETC inhibitors), and measuring the OCR after each successive addition (Fig. 5A, B for mid-exponential and stationary growth phases respectively). Key glycolytic fluxes (basal glycolytic rate, glycolytic capacity, glycolytic reserve and non-glycolytic acidification) were determined according to TeSlaa and Teitell (2014) by combining the sequential effects of optimized concentrations of glucose (glycolysis induction), oligomycin (ATP synthase inhibition) and 2-deoxy-D-glucose (glycolysis inhibition) with measurement of ECAR after each successive addition (Fig. 6A, B for mid-exponential and stationary growth phases respectively). Microplate assays were initiated in fresh XF DMEM medium containing glucose (16.74 mM) and glutamine (2 mM) for mitochondrial determinations or glutamine (2 mM) for glycolysis. To directly compare biomass-specific mitochondrial and glycolytic functions, all measurements were normalized using cell number and then corrected using a subclone-specific mean cell volume factor.

Mitochondrial function

Comparative analysis of cells sampled from mid-exponential phase (Fig. 5A) and stationary phase (Fig. 5B) cultures revealed few conserved and significant culture phase specific differences in mitochondrial respiratory control. The increase in non-mitochondrial respiration (Fig. 5H) may be derived from an increased activity of various enzymes that consume oxygen (e.g. NADPH oxidases, desaturases and detoxification enzymes; (Brand and Nicholls 2011) or cell surface oxygen consumption via trans-plasma membrane electron transport (Herst and Berridge 2007) and may explain the increased basal oxygen consumption of some stationary phase subclones (Fig. 5C).

In contrast, comparing subclone groups with different FBC biomass performance (Fig. 3) and despite inherent clonal variation, we observed substantial differences in mitochondrial functions measured. The only (relatively small) difference in mitochondrial function evident for cells sampled during exponential phase culture was an increased mitochondrial coupling efficiency (the fraction of basal oxygen consumption used for ATP synthesis) of higher biomass performance cells (Fig. 5I) with a similar trend towards increased ATP turnover (Fig. 5D). Given the absence of any differences in proton leak (Fig. 5G; a strong indicator of mitochondrial dysfunction), this implies that mitochondria in exponential phase higher biomass performance cells are capable of more efficient ATP production at similar or mildly increased basal respiration rates (Fig. 5C) and that this may be associated with increased growth rate during exponential phase culture (Fig. 2E). Moreover, these subclones were able to maintain mitochondrial ATP production with evidence of generally reduced spare respiratory capacity (Fig. 5F) without increased uncoupled maximal respiration rate (Fig. 5E). Together, we infer that high performance subclones may achieve high cell specific growth rate during exponential phase culture via higher efficiency use of available mitochondrial biomass.

Differences in mitochondrial respiratory control between subclone groups differing in FBC biomass were most evident for cells sampled from stationary phase cultures. High performance cells sampled from stationary phase cultures exhibited elevated basal respiration (oxygen consumption, Fig. 5C), ATP production (Fig. 5D), proton leak (Fig. 5G), maximal (uncoupled) respiration (electron transport uncoupled from mitochondrial oxygen consumption, Fig. 5E) and spare respiratory capacity (ability of substrate supply and electron transport to respond to an increase in energy demand, Fig. 5F) all normalized with respect to cell biomass. Importantly, these data clearly reveal a culture phase specific up-regulation of mitochondrial oxidative capacity specifically associated with the higher performance subclone groups and this is proportionate to late stage culture performance (Fig. 3C). The increase in proton leak (Fig. 5G) is proportionate to the increase in other mitochondrial functional measurements for cells sampled at stationary phase. Together these data imply that high late stage culture performance may be associated with increased mitochondrial biogenesis (LeBleu et al. 2014) and/or decreased mitochondrial protein turnover (Kitami et al. 2012) through culture rather than a de-repression of pre-existing mitochondrial biomass, e.g. via alleviation of a glucose induced inhibition of mitochondrial oxidation (the Crabtree effect; Diaz-Ruiz et al. (2011)), or the maintenance of a Crabtree effect in subclones exhibiting poor late stage culture performance. However, this is a relatively rare and possibly transient cellular phenotype, where subclonal evolution towards rapid exponential proliferation is, in general, inversely proportional to late stage culture performance (Fig. 2D).

Glycolysis/ECAR

As per mitochondrial respiratory control, comparative analysis of cells sampled from mid-exponential phase (Fig. 6A) and stationary phase (Fig. 6B) cultures generally revealed highly conserved culture phase specific differences in glycolytic function. Generally, stationary phase

cells exhibited elevated measurements of glycolytic reserve (Fig. 6E), which is glycolytic rate from supplied glucose (effectively ECAR deriving from lactate production) subtracted from glycolytic rate after inhibition of mitochondrial ATP synthesis by oligomycin (glycolytic capacity, Fig. 6D). Thus, these data indicate that although glycolytic flux in exponential phase cells likely proceeds unconstrained at maximum capacity, a regulatory link between glycolytic flux to lactate and mitochondrial ATP synthesis exists in stationary phase cells generally. This is indicative of a fundamental alteration in metabolic programming towards a general reliance on oxidative metabolism as culture progresses. Secondly, the general increase in non-glycolytic acidification (in the unbuffered media without glucose, Fig. 6F) can derive from TCA cycle CO₂ production (Divakaruni et al. 2013) or possibly via lactate derived from conversion of cytosolic malate to pyruvate, indicating significantly enhanced potential for glutamine-(or other amino acid) stimulated mitochondrial oxidation in stationary phase cells.

Comparing subclone groups with different FBC performance (Fig. 3), we observed clear differences in ECAR. High-performance subclones sampled at exponential phase exhibited relatively low glycolytic rates (Fig. 6C) and glycolytic capacities (Fig. 6D) in the assay medium containing glucose and glutamine (analogous to minimally conditioned medium during early stage culture). This contrasts markedly with the significantly higher glycolytic rates and capacities of the same subclones sampled during stationary phase. Moreover, high-performance subclones sampled at stationary phase also exhibited a higher glycolytic reserve (Fig. 6E) and non-glycolytic ECAR (Fig. 6F).

Taken together these observations reveal that high-performance subclones (i) are likely less reliant on glucose for rapid exponential phase proliferation, in accord with their higher glutamine uptake rate during FBC (Fig. 4C), (ii) maintain the potential for significantly higher glycolytic function in late stage culture relative to other cells sampled at stationary phase (Fig. 6C-E; and also compared to their own glycolytic function when sampled during exponential

phase), (iii) can couple high glycolytic capacity with high mitochondrial oxidation and ATP synthesis capacity per unit biomass (Fig. 5), revealing a distinctly different central metabolic functional competency to support anabolism during late stage culture.

However, we observed that high-performance cells exhibit reduced glucose consumption during late stage FBC relative to other cells with no difference in glutamine consumption (which was not supplied in feeds and effectively exhausted; Fig. 4). Thus, we infer that their inherently increased metabolic and oxidative capacity can be supported by increased uptake and utilization of other amino acids and/or fatty acids to support anaplerosis. We also note that late stage FBC medium had a high extracellular lactate concentration (up to 30 mM) compared to that present in glycolytic and mitochondrial assays in fresh medium where lactic acidosis may itself prevent glycolysis (Leite et al. 2011; Mulukutla et al. 2012).

Functional characterization of high-performance cells by transient production of easy-to-express and difficult-to-express recombinant proteins

To determine if the increased ability of high-performance subclones (1.80, 2.200, 4.200, 11.80 and 17.200) to produce and maintain cell biomass could be harnessed to support increased recombinant protein production we compared production of both an “easy-to-express” (ETE) recombinant protein (secreted embryonic alkaline phosphatase; SEAP) and a “difficult-to-express” (DTE) Sp35Fc fusion protein (Johari et al. 2015) in an optimized fed-batch transient production mode mediated by lipofection. Although the use of transient expression to compare clone production “capacity” has inherent limitations (e.g. variation in clone-specific “transfectability”, progressive dilution of plasmid copy number during cell proliferation), it does permit a rapid evaluation of the relative ability of cell populations to create product from an equivalent “load” of transfected plasmid DNA and of specific importance for a DTE protein

known to induce the UPR (Johari et al. 2015), the extent to which capacity for cell growth is inhibited by recombinant protein production. These data are shown in Fig. 7.

Compared to control parental cells all evolved, biomass intensive cell lines exhibited increased volumetric titer of SEAP after 9 days culture (from 1.19 to 1.92-fold; Fig. 7A), and all except clone 2.200 exhibited increased an volumetric titer of Sp35Fc (from 1.16 to 1.52-fold; Fig. 7B). All clones except 2.200 exhibited an increased IVCC and IVCV as expected. However, the extent of the increase in IVCC and IVCV was more pronounced for cells expressing the DTE protein Sp35Fc (1.36 and 1.41-fold, respectively) than for cells expressing the ETE protein SEAP (1.28 and 1.32-fold, respectively). Cell specific production rates were clone-specific. Interestingly, subclone 1.80 attained the highest increase in product titer for both recombinant proteins by mostly an increase in qP (indicating a “biomass-dominant” phenotype) whereas subclone 17.200 which attain a very high IVCC displayed a reduced qP (indicating a “proliferation-dominant” phenotype). From these data, we infer that the increased ability of evolved cells to create and maintain cell biomass does generally support increased productive capacity and minimize the anti-proliferative effect of the UPR-inducing DTE protein Sp35Fc. Moreover, we infer that if stably transfected, evolved cells would exhibit greater increases in product titer as the effect of diluted plasmid copy number after transient transfection would be absent.

DISCUSSION

Response to the selective pressure: balancing cell biomass and exponential proliferation

As cells increase exponential growth rate during evolutionary subculture, average CHO cell volume/biomass declines proportionately. This inverse relationship between cell volume and growth rate is typical both for CHO cells (Davies et al. 2012; Kang et al. 2014) and for other transformed cells in culture (Dolfi et al. 2013). The extended subculture regime we employed

created CHO cell lineages varying in their relationship between cell size and cell proliferation. Assuming a continued linear increase in specific growth rate (Fig. 1), further continuous subculture could have extended the phenotype towards even smaller cell size – ultimately towards the physical constraints imposed, for example, by correct functioning of the mitotic apparatus (Marshall et al. 2012). Considering all evolved cells, this evolutionary process does not generally yield subclonal populations that make more total cell biomass per unit time (IVCV), but selects for cells that presumably commit to entry into mitosis earlier in G1, reducing average cell size. The cell/molecular biological control mechanisms underpinning this change in homeostatic coupling of cell size and proliferation are not yet elucidated. Recent studies have established that mammalian cell division varies independently with cell size and age (Tzur et al. 2009), and direct observations of mammalian cell growth in microfluidic chambers suggest that cell growth rate varies through the cell cycle, where cells are required to achieve a growth rate threshold (gate) to enter into the G1-S transition (Son et al. 2012). The most complete mechanistic understanding of cell size control comes from studies of fission and budding yeasts which suggests that cells utilize a variety of sensing mechanisms to measure their own size and rate of biomass accumulation which regulate the timing of cell division (Marshall et al. 2012). Few genetic engineering strategies to increase CHO cell size and growth rate have been reported. Dreesen and Fussenegger (2011) employed ectopic expression of the metabolic sensor mTOR (mammalian target of rapamycin) to improve the capacity of engineered CHO cells to produce different recombinant proteins. More recently McVey et al. (2016) showed that knock-out of the mTORC1 inhibitor TSC2 resulted in increased cell size and specific production rate. Importantly however, the effects of TSC2 knockout were parental clone specific, and resulted in reduction of cell proliferation rate and peak cell density.

Therefore, we utilized multiparallel evolution of subclonal populations to derive diverse metabolic phenotypes varying in ability to proliferate and create cellular biomass

Accepted Preprint

during a fed-batch process. We hypothesized that evolved, rapidly proliferating smaller cells would acquire differences in transcriptional and metabolic programming to larger cells proliferating more slowly. At the most basic level, assuming cellular DNA content remains constant, then smaller, more rapidly dividing cells acquire a progressively higher DNA: cell biomass ratio, with a larger surface to volume ratio. Accordingly, we may reasonably expect conserved differences in global and specific transcriptional output (Marguerat and Bähler 2012) associated with variations in total biomass synthesis rate and biomass composition. For example, Pires das Neves et al. (2010) showed that due the asymmetric partitioning of mitochondria during mitosis, HeLa cells with a higher mitochondrial mass exhibited a higher global transcription and proliferation rates. They proposed that elevated ATP content activates RNA polymerase II. More recently, an elegant study by Miettinen et al. (2014) comparing hepatocytes of varying size (created by decoupling growth and proliferation on ablation of cyclin-dependent kinase 1, such that μ was inversely proportional to cell size), revealed that the expression of mitochondrial and lipid synthesis genes was downregulated in larger cells. The authors associated this with a lower requirement for lipid membrane components, where accumulated excess lipids would inhibit lipid biosynthesis and mitochondrial metabolism. Thus, our hypothesis was generally correct, but with some caveats – most specifically concerned with the genetic stability of evolving transformed cell populations. Our data shows that evolutionary subculture is necessary to create CHO cell sub-populations with a markedly different and relatively uncommon metabolic program that supports superior FBC performance. However, this advantageous metabolic program arises from, and is subject to, genetic/functional drift; our data suggest that evolution is necessary to create new metabolic programs, but that these are infrequent. Most cells that acquired the ability to proliferate rapidly also acquired poor late stage culture performance.

Functional variation between and within subcultures, unsurprisingly, was pervasive. Genetic instability and drift within populations enabled subclones to re-program their metabolism and morphology to adapt to the selective pressure (Beckmann et al. 2012; Davies et al. 2012; Merlo et al. 2006). From an evolutionary perspective, to achieve rapid proliferation the genome evolves a cellular environment that can more rapidly utilize extracellular precursors to create the minimal amount of machinery necessary to replicate itself. This objective is likely achieved, in most cases, at the expense of genome fidelity, as the burden of genome surveillance and repair would render cells which rigorously undertook these processes uncompetitive within the population (Gorringe et al. 2005; Stopper et al. 2003). Hence, chromosomal variants and point mutations accumulate within isolated genetically drifting populations. Genetic and functional stability is rare. This is a hallmark of transformed cancer cells, which also exhibit this phenomenon (Gorringe et al. 2005). Only two of our 22 clonal isolates (subclones 4 and 13; Fig. 2C, D) proved functionally stable during extended subculture, one of which exhibited high FBC performance (subclone 4). We infer that the functional stability of these “antimutators” arises from their intrinsic genomic stability, which is provided by processes such as DNA mismatch repair during genome replication which is defective in many cancers (Bak et al. 2014). Arguably therefore, although subclone 1.80 exhibited superior manufacturing performance (Fig. 7), the functionally stable subclone 4 may be a better choice for a parental CHO host cell line. Whether this ideal set of properties would be carried forward into a new generation of stable transfectants engineered to produce recombinant proteins is an open question. Previous reports of “bioreactor evolved” CHO cell hosts (Prentice et al. 2007) would suggest that this is possible. This may be a more desirable objective phenotype as it may be possible to stack additional traits into an inherently stable genomic environment for more predictable performance characteristics.

Variation in metabolic phenotypes associated with exponential growth rate

For the majority of subclones, as serial subculture progressed late stage culture performance declined as increased exponential growth rate increased, especially after 80 generations (Fig. 2C, D). This inverse relationship could imply a simple progressive general limitation in conditioned medium sufficiency or inhibitory metabolite accumulation were it not for the group of high FBC performance subclones (Fig. 3A) that disprove this generality. Indeed, some subclones (e.g. subclones 2, 17) exhibited the opposite trend – increasing both proliferation and late stage culture performance during evolution. Remarkably, for subclones that did exhibit (albeit transiently) relatively high FBC performance, we observed highly conserved differences in core metabolic functions. Specifically, (i) relatively high glutamine consumption and lactate production during exponential growth coupled with more efficient mitochondrial oxidative ATP production and reduced glycolytic flux, (ii) significantly higher mitochondrial and glycolytic capacity available at the onset of stationary phase associated with significantly higher late stage culture performance. Together, these data imply that high performance CHO subclones utilize a distinct metabolic program that enables them to respond to the competitive selective pressure (growth rate) but also does not disable (or enhances) late stage culture performance. How can we rationalize these observations? Recent advances in knowledge of cancer cell metabolism may provide some insights. It is now well known that a hallmark of cancer cell metabolism is a reliance on glucose as a primary fuel to support aerobic glycolysis to lactate (Warburg 1956) and glutamine as a carbon and nitrogen source for anaplerosis and redox homeostasis (Hensley et al. 2013; Vander Heiden et al. 2009). The best characterized metabolic phenotype of tumor cells is a shift from ATP production via mitochondrial OXPHOS to aerobic glycolysis, where the mitochondrial TCA cycle becomes an important source of precursors for anabolism, such as citrate for lipid biosynthesis. PI3K/AKT1, HIF, p53, MYC and AMPK kinase have been implicated in metabolic re-programming of cancer cells towards

aerobic glycolysis which is itself an important source of precursors for anabolism via, for example, the oxidative pentose phosphate pathway to generate NADPH (for macromolecular biosynthesis and redox control) and nucleotides. In this respect allosteric regulation of the M2 isoform of pyruvate kinase (PKM2), prevalent in transformed cells, has also been identified as a key effector which can, in its inactive dimeric form, shift flux of pyruvate to lactate and pool glycolytic intermediates to support anabolic pathways (Dong et al. 2016; Wong et al. 2013).

Therefore, in the context of our data, the reduced exponential phase glycolytic capacity and increased glutamine uptake of high performance FBC cells suggest the use of a different, more flexible metabolic program that is characterized by conserved features. Firstly, an increased metabolic dependency on glutamine to support proliferation. In this case glutamine (via glutamate) could be utilized for anaplerosis directly, feed into the serine/glycine biosynthetic pathway to support protein, glutathione and nucleotide biosynthesis – a pathway central to cancer cell proliferation (Jain et al. 2012; Yang and Vousden 2016) and/or undergo reductive carboxylation by IDH1 to citrate to fuel lipid biosynthesis (Metallo et al. 2012). Mutational events that could support enhanced glutaminolysis have been reported. Most cited is the influence of MYC, which increases cell proliferation and the expression of genes that promote glutamine uptake and catabolism (Cairns et al. 2011; Hensley et al. 2013). More recently, Ma et al. (2013) have also reported that loss of PKC ζ expression can reprogram cancer cell metabolism to utilize glutamine via the serine pathway during nutrient stress. Associated with this mid- to high performance cells capable of increased exponential growth rate exhibited reduced glycolytic capacity in microplate assay conditions, where all mid- to high performance cells apparently operated at maximum glycolytic capacity during this phase as oligomycin (Fig. 6D), which uncouples ATP synthesis by mitochondrial OXPHOS, did not further elevate ECAR. In fact, the negative glycolytic reserve derived for the majority of mid- and high-performance cells may relate to their additional reliance on mitochondrial ATP production and

raises the possibility that these cells may have an additional capacity to resorb secreted lactate or pyruvate such that their basal “net” ECAR (Fig. 6C) is lowered. Thus, the data in Fig. 4, which show that actual FBC glucose consumption (Fig. 4A) measured during the same phase of FBC were generally equivalent can be reconciled. The increased exponential FBC lactate production (Fig. 4B) by high-performance cells may relate to the different culture conditions between microplate assay and conditioned media in FBC. We do not discount the possibility that a proportion of the ECAR we observed in the microplate assay conditions (Fig. 6B) may also be due to secretion of pyruvate itself rather than lactate, which is commonly secreted by cancer cells (Hong et al. 2016; Jain et al. 2012). Also, FBC may also generate lactate from sources other than glycolysis, for example pyruvate may be derived from malate via malic enzyme, where glutamine (and potentially other amino acids), which may function as an anaplerotic substrate in high-performance cells, is at a significantly higher concentration in CD-CHO medium used for FBC (8 mM) than in the medium utilized for the microplate assay (2 mM). Indeed, intracellular lactate has itself been shown to promote glutamine uptake by oxidative cancer cells (Pérez-Escuredo et al. 2016).

It is clear that relatively high lactate production *per se* did not impede the exponential proliferation (nor subsequent late stage culture) of high-performance cells. It may be the case that high lactate production and export is actually advantageous for rapid proliferation not just as a means to recycle NAD^+ , but also to avoid accumulation of ROS as inactivation of LDHA in cancer cells has been shown to lead to ROS accumulation possibly via feedback effects on glycolysis (Doherty and Cleveland 2013; Le et al. 2012). Moreover, inhibition of monocarboxylate transporters that export lactate and pyruvate is currently under investigation as a promising means to block cancer cell growth (Doherty et al. 2014; Hong et al. 2016). Although we did not measure pyruvate concentrations, we speculate that accumulated pyruvate during late stage culture could be a readily available nutrient source for oxidative metabolism

and/or gluconeogenesis to support high-performance cells during late stage culture as previously described for CHO cells (Li et al. 2012; Sellick et al. 2011). Lactate consumption, rather than residual glucose or lactate concentrations, has been shown to be a strong indicator of production performance (Le et al. 2012). The fact that pH was not controlled during our shake-flask FBC model may also be of significance. Extracellular pH can itself affect metabolism; recent studies on hybridomas have shown that reduced pH (6.8) induced lactate import and shifted cells to a more energy efficient state with respect to ATP production, increasing MAb production (Ivarsson et al. 2015). Similarly, Liste-Calleja et al. (2015) shown that the metabolic shift to lactate consumption on HEK cells is triggered at reduced pH levels (6.8) as a strategy for pH detoxification. Furthermore, we speculate that the relative ability of cells to maintain proliferation and viability with limited external pH control may itself contribute to their high FBC performance. Cells utilize a variety of mechanisms to achieve intracellular pH homeostasis (Casey et al. 2010), and CHO cells in a metabolic culture environment able to exert intracellular and environmental homeostatic pH control mechanisms, regulating exchange of metabolites and ions to optimize maintenance of biomass may have an inherent advantage. For some clones it may not be necessary (and even a metabolic constraint) to control extracellular pH within narrow bounds. A hallmark of cancer cells is an ability to sense, adapt and control environmental pH (Swietach et al. 2014).

High performance cells (as well as maximally evolved cells with high specific growth rate) exhibited a generally increased efficiency of mitochondrial OXPHOS during exponential growth. Without increasing mitochondrial capacity, ATP production is sustained by a high coupling efficiency (of O₂ consumption to ATP production) and reduced spare OXPHOS capacity. Thus our data support a general conclusion that maximal growth rates are associated with the evolutionary acquisition of mitochondrial functional integrity to support OXPHOS (e.g. Fig. 3B, Fig. 5D, I), and that this is a necessary but not sufficient prerequisite for increased

late stage culture performance. Recent studies have also highlighted the wide diversity of mitochondrial functional states within tumors and between transformed cell lines (Zheng 2012). For example, Warburg considered that dysfunctional mitochondria are required for aerobic glycolysis (Senyilmaz and Teleman 2015). Whilst this association may be the case in some cancer cells (e.g., López-Ríos et al. (2007), Owens et al. (2011)), others report intact mitochondrial OXPHOS in cancer cells (e.g., Fantin et al. (2006), Scott et al. (2011), Smolková et al. (2011)). Additionally, metabolic reliance on either glycolysis or OXPHOS can vary with prevailing environmental conditions. For example, OXPHOS is reported to provide 79 or 91% of ATP in HeLa and breast MCF cells respectively, which is reduced to 29 and 36% in hypoxia (Rodríguez-Enríquez et al. 2010). Aerobic glycolysis is not a universal feature of all proliferating cancer cells; they can exhibit considerable metabolic flexibility (Cairns et al. 2011) in the use of amino acids, lipids or lactate as fuels (DeBerardinis et al. 2008; Sonveaux et al. 2008; Yang et al. 2009). Our data support the conclusion that oxidative ATP production by mitochondria necessarily supports both rapid proliferation and late stage culture performance and that continued passaging of cells may represent an indirect selection process for OXPHOS. Of course we expect frequent mutations in CHO mitochondrial genes occur that can alter mitochondrial bioenergetics and the interaction with host cell signaling pathways, oncogenes, metabolism (e.g. ROS formation/degradation) that regulate mitochondrial function (Wallace 2012).

Variation in metabolic phenotypes associated with late stage culture performance

A minority of subclonal populations acquired significantly improved late stage culture performance during serial subculture. Associated with this there was strong evidence of a substantial shift in metabolic programming when mitochondrial and glycolytic functions were assayed at the onset of stationary phase in the same microplate format. Importantly, the

unconditioned media environment of the microplate assay, albeit common across all cells, was distinctly different to the conditioned media environment from which the cells were sampled. Nevertheless, significant and conserved differences were observed, high performance cells exhibited both increased oxidative mitochondrial respiratory function and glycolytic activity (Fig. 5 and 6). These data confirm previous analyses of metabolic flux in engineered CHO cell lines selected for high FBC productivity which report that maximal MAb production during stationary phase is associated with energy generation via OXPHOS and elevated oxidative pentose phosphate pathway activity (Ahn and Antoniewicz 2011; Sengupta et al. 2011; Templeton et al. 2013). Supporting this, another flux balance analysis showed that late stage culture CHO cells consuming lactate have an energy efficiency (*per* C-mol of substrate consumed) six times greater than lactate producing cells (Martinez et al. 2013).

The intricate cellular controls which enable this metabolic re-programming in some subclones but not others are not yet determined, but likely involve central regulators of cellular ATP homeostasis such as AMPK (Hardie 2014) that is known to activate mitochondrial biogenesis via PGC-1 α , and SIRT1, a nutrient deprivation sensor that also activates PGC-1 α (Hock and Kralli 2009; Scarpulla 2011). The PGC family of coactivators (PGC-1 α , PGC-1 β and PRC) have been identified as predominant transcriptional regulators of mitochondrial function and biogenesis (Scarpulla 2011; Scarpulla et al. 2012) that are likely to coordinate synthesis of increased mitochondrial oxidative capacity in stationary phase high performance CHO cells. Upstream of (or in addition to) PGC coactivators, other transcription factors have been implicated in control of mitochondrial biogenesis and function, for example, CREB, MYC, OCT and YY1 (Hock and Kralli 2009; Jose et al. 2011; Scarpulla et al. 2012) which may all be involved in regulatory control mechanisms. Activation of mitochondrial oxidative capacity at stationary phase is likely to be closely associated with an energy-dependent regulation, since the limiting glutamine availability (glutamine levels were almost depleted at

stationary phase, data not shown) reduces both anaplerotic reactions and energy levels. This restriction can modulate the expression of PGC-1 α via either AMPK (Chaube et al. 2015) or SIRT-1 activation (Dominy and Puigserver 2013), resulting in increased mitochondrial biogenesis and the OXPHOS capacity (LeBleu et al. 2014). In addition to this, cells may then utilize other carbon/nitrogen sources (e.g., asparagine and other branched chain amino acids) as anaplerotic substrates.

The increase in glycolytic capacity we observed in stationary phase high performance cells is also likely to involve networks of transcription factors and signaling proteins acting in concert. For example, upregulation of glycolytic machinery in cancer cells is typically associated with downregulation of mitochondrial oxidative machinery. Oncogenic Ras mutations are often found in cancer cells which drive cells towards aerobic glycolysis via activation of the PI3K-Akt-mTOR pathway. mTOR can induce HIFs (hypoxia inducible transcription factors), which can induce many genes including glucose transporters and glycolytic enzymes (Zheng 2012). However other transcription factors such as MYC and p53 may also play a role, where for example HIFs have been reported to both repress MYC activity (Zhang et al. 2007) and promote MYC transcription and cooperate with MYC in increasing glycolysis (Dang et al. 2008). Other layers of cellular control may also be functionally relevant. For example, MYC is reported to enhance mitochondrial metabolism via suppression of miR-23a/b (Gao et al. 2009). Suppression of miR-23 activity in CHO cells has recently been reported to both increase mitochondrial activity and recombinant reporter protein production (Kelly et al. 2015). Lastly, despite evidence of metabolic reprogramming of high performance cells towards increased glycolytic capacity at the onset of stationary phase (Fig. 6), this was not actually associated with increased glucose uptake (Fig. 4). This may imply a substrate level control mechanism: Intracellular lactate itself may inhibit glycolysis via inhibition of hexokinase and phosphofructokinase (Leite et al. 2011; Mulukutla et al. 2012) thus repressing

the import of glucose into cells in conditioned media during FBC, but not cells in fresh, lactate-free media in the microplate assay. Moreover, independent of glycolytic flux, an increased glycolytic enzyme capacity may also support a variety of non-glycolytic functions, such as activation of survival pathways, cell cycling and transcription etc. (Lincet and Icard 2015).

In summary, a detailed understanding of the coordinated signaling pathways and oncogenes that dynamically control mitochondrial and metabolic capacity will be necessary, in conjunction with metabolic flux modeling, to enable not just optimization of flux to cell/product biomass through a generic CHO metabolic network, but optimal organization and capacity of the cellular network itself. We suggest that given the likely complexity and inherent variability of cellular control mechanisms in CHO cells (and cancer cells generally) that together contribute to the ideal (rapidly proliferating, biomass intensive, stable) CHO production phenotype, successful cell engineering strategies to achieve this objective are unlikely to be based on a small number of genetic alterations, even of those targets that affect many downstream processes (e.g. signaling nodes, transcription factors, miRNAs). If possible, this would likely require more sophisticated, coordinated control of the expression of multiple gene products simultaneously at an appropriate stoichiometry (Brown and James 2016). At present this multigenic cell engineering goal, to unlock the biosynthetic capacity of CHO cells, is more likely to be achievable via alternative strategies such as directed evolution (e.g. Prentice et al. (2007)) using appropriate selective environments that permit cells to achieve coordinated/balanced genome engineering (Birchler and Veitia 2012; Lee et al. 2014) underpinning the desired phenotype. In this respect, it would be possible to utilize the inherent genetic instability of CHO cells advantageously, balancing instability against evolutionary gain (Schubert and Vu 2016).

Acknowledgements

This research was made possible by financial support from The University of Sheffield and CONACYT. The authors gratefully thank Biogen for providing the Sp35Fc gene.

REFERENCES

- Ahn WS, Antoniewicz MR. 2011. Metabolic flux analysis of CHO cells at growth and non-growth phases using isotopic tracers and mass spectrometry. *Metab Eng.* 13(5):598-609.
- Ahn WS, Antoniewicz MR. 2013. Parallel labeling experiments with 1,2-C-13 glucose and U-C-13 glutamine provide new insights into CHO cell metabolism. *Metab Eng.* 15:34-47.
- Bak ST, Sakellariou D, Pena-Diaz J. 2014. The dual nature of mismatch repair as antimutator and mutator: for better or for worse. *Front Genet.* 5:287.
- Beckmann TF, Kramer O, Klausning S, Heinrich C, Thute T, Buntemeyer H, Hoffrogge R, Noll T. 2012. Effects of high passage cultivation on CHO cells: a global analysis. *Appl Microbiol Biotechnol.* 94(3):659-671.
- Birchler JA, Veitia RA. 2012. Gene balance hypothesis: connecting issues of dosage sensitivity across biological disciplines. *Proc Natl Acad Sci U S A.* 109(37):14746-14753.
- Brand MD, Nicholls DG. 2011. Assessing mitochondrial dysfunction in cells. *Biochem J.* 435:297-312.
- Brown AJ, James DC. 2016. Precision control of recombinant gene transcription for CHO cell synthetic biology. *Biotechnol Adv.* 34(5):492-503.
- Cairns RA, Harris IS, Mak TW. 2011. Regulation of cancer cell metabolism. *Nat Rev Cancer.* 11(2):85-95.
- Casey JR, Grinstein S, Orlowski J. 2010. Sensors and regulators of intracellular pH. *Nat Rev Mol Cell Biol.* 11(1):50-61.
- Chaube B, Malvi P, Singh SV, Mohammad N, Viollet B, Bhat MK. 2015. AMPK maintains energy homeostasis and survival in cancer cells via regulating p38/PGC-1 α -mediated mitochondrial biogenesis. *Cell Death Discov.* 1:15063.
- Dang CV, Kim J-w, Gao P, Yustein J. 2008. The interplay between MYC and HIF in cancer. *Nat Rev Cancer.* 8(1):51-56.
- Davies SL, Lovelady CS, Grainger RK, Racher AJ, Young RJ, James DC. 2012. Functional heterogeneity and heritability in CHO cell populations. *Biotechnol Bioeng.* 110(1):260-274.
- DeBerardinis RJ, Mancuso A, Daikhin E, Nissim I, Yudkoff M, Wehrli S, Thompson CB. 2007. Beyond aerobic glycolysis: Transformed cells can engage in glutamine metabolism that exceeds the requirement for protein and nucleotide synthesis. *Proc Natl Acad Sci USA.* 104(49):19345-19350.

- DeBerardinis RJ, Sayed N, Ditsworth D, Thompson CB. 2008. Brick by brick: metabolism and tumor cell growth. *Curr Opin Genet Dev.* 18(1):54-61.
- Diaz-Ruiz R, Rigoulet M, Devin A. 2011. The Warburg and Crabtree effects: On the origin of cancer cell energy metabolism and of yeast glucose repression. *Biochim Biophys Acta.* 1807(6):568-576.
- Divakaruni A, Paradyse A, Ferrick D, Murphy A, Jastroch M. 2013. Analysis and interpretation of microplate-based oxygen consumption and pH data. *Methods Enzymol.* 547:309-354.
- Doherty JR, Cleveland JL. 2013. Targeting lactate metabolism for cancer therapeutics. *J Clin Invest.* 123(9):3685-3692.
- Doherty JR, Yang C, Scott KE, Cameron MD, Fallahi M, Li W, Hall MA, Amelio AL, Mishra JK, Li F. 2014. Blocking lactate export by inhibiting the Myc target MCT1 disables glycolysis and glutathione synthesis. *Cancer Res.* 74(3):908-920.
- Dolfi SC, Chan LL, Qiu J, Tedeschi PM, Bertino JR, Hirshfield KM, Oltvai ZN, Vazquez A. 2013. The metabolic demands of cancer cells are coupled to their size and protein synthesis rates. *Cancer Metab.* 1(1):20.
- Dominy JE, Puigserver P. 2013. Mitochondrial biogenesis through activation of nuclear signaling proteins. *Cold Spring Harb Perspect Biol.* 5(7):a015008.
- Dong G, Mao Q, Xia W, Xu Y, Wang J, Xu L, Jiang F. 2016. PKM2 and cancer: The function of PKM2 beyond glycolysis (Review). *Oncol Lett.* 11(3):1980-1986.
- Dorai H, Kyung YS, Ellis D, Kinney C, Lin C, Jan D, Moore G, Betenbaugh MJ. 2009. Expression of Anti-Apoptosis Genes Alters Lactate Metabolism of Chinese Hamster Ovary Cells in Culture. *Biotechnol Bioeng.* 103(3):592-608.
- Dreesen IAJ, Fussenegger M. 2011. Ectopic Expression of human mTOR Increases Viability, Robustness, Cell Size, Proliferation, and Antibody Production of Chinese Hamster Ovary Cells. *Biotechnol Bioeng.* 108(4):853-866.
- Fantin VR, St-Pierre J, Leder P. 2006. Attenuation of LDH-A expression uncovers a link between glycolysis, mitochondrial physiology, and tumor maintenance. *Cancer cell.* 9(6):425-434.
- Frame KK, Hu WS. 1990. Cell volume measurement as an estimation of mammalian cell biomass. *Biotechnol Bioeng.* 36(2):191-197.
- Gao P, Tchernyshyov I, Chang T-C, Lee Y-S, Kita K, Ochi T, Zeller KI, De Marzo AM, Van Eyk JE, Mendell JT. 2009. c-Myc suppression of miR-23a/b enhances mitochondrial glutaminase expression and glutamine metabolism. *Nature.* 458(7239):762-765.

- Gorringer KL, Chin S-F, Pharoah P, Staines JM, Oliveira C, Edwards PA, Caldas C. 2005. Evidence that both genetic instability and selection contribute to the accumulation of chromosome alterations in cancer. *Carcinogenesis*. 26(5):923-930.
- Hardie DG. 2014. AMP-activated protein kinase: maintaining energy homeostasis at the cellular and whole-body levels. *Annu Rev Nutr*. 34:31-55.
- Hensley CT, Wasti AT, DeBerardinis RJ. 2013. Glutamine and cancer: cell biology, physiology, and clinical opportunities. *J Clin Invest*. 123(9):3678-3684.
- Herst PM, Berridge MV. 2007. Cell surface oxygen consumption: a major contributor to cellular oxygen consumption in glycolytic cancer cell lines. *Biochim Biophys Acta*. 1767(2):170-177.
- Hock MB, Kralli A. 2009. Transcriptional control of mitochondrial biogenesis and function. *Annu Rev Physiol*. 71:177-203.
- Hong CS, Graham NA, Gu W, Camacho CE, Mah V, Maresh EL, Alavi M, Bagryanova L, Krotee PA, Gardner BK. 2016. MCT1 modulates cancer cell pyruvate export and growth of tumors that co-express MCT1 and MCT4. *Cell reports*. 14(7):1590-1601.
- Ivarsson M, Noh H, Morbidelli M, Soos M. 2015. Insights into pH-induced metabolic switch by flux balance analysis. *Biotechnol Prog*. 31(2):347-357.
- Jain M, Nilsson R, Sharma S, Madhusudhan N, Kitami T, Souza AL, Kafri R, Kirschner MW, Clish CB, Mootha VK. 2012. Metabolite profiling identifies a key role for glycine in rapid cancer cell proliferation. *Science*. 336(6084):1040-1044.
- Johari YB, Estes SD, Alves CS, Sinacore MS, James DC. 2015. Integrated cell and process engineering for improved transient production of a "difficult-to-express" fusion protein by CHO cells. *Biotechnology and Bioengineering* 112(12):2527-2542.
- Jose C, Bellance N, Rossignol R. 2011. Choosing between glycolysis and oxidative phosphorylation: a tumor's dilemma? *Biochim Biophys Acta*. 1807(6):552-561.
- Kang S, Ren D, Xiao G, Daris K, Buck L, Enyenihi AA, Zubarev R, Bondarenko PV, Deshpande R. 2014. Cell line profiling to improve monoclonal antibody production. *Biotechnol Bioeng*. 111(4):748-760.
- Kelly PS, Breen L, Gallagher C, Kelly S, Henry M, Lao NT, Meleady P, O'Gorman D, Clynes M, Barron N. 2015. Re-programming CHO cell metabolism using miR- 23 tips the balance towards a highly productive phenotype. *Biotechnol J*. 10(7):1029-1040.
- Kitami T, Logan DJ, Negri J, Hasaka T, Tolliday NJ, Carpenter AE, Spiegelman BM, Mootha VK. 2012. A chemical screen probing the relationship between mitochondrial content and cell size. *PloS one* 7(3):e33755.

- Le H, Kabbur S, Pollastrini L, Sun Z, Mills K, Johnson K, Karypis G, Hu WS. 2012. Multivariate analysis of cell culture bioprocess data--lactate consumption as process indicator. *J Biotechnol. Netherlands*: 2012 Elsevier B.V. p 210-23.
- LeBleu VS, O'Connell JT, Herrera KNG, Wikman-Kocher H, Pantel K, Haigis MC, De Carvalho FM, Damascena A, Chinen LTD, Rocha RM. 2014. PGC-1alpha mediates mitochondrial biogenesis and oxidative phosphorylation in cancer cells to promote metastasis. *Nat Cell Biol.* 16(10):992.
- Lee YW, Gould BA, Stinchcombe JR. 2014. Identifying the genes underlying quantitative traits: a rationale for the QTN programme. *AoB Plants.* 6(0):plu004.
- Leite TC, Coelho RG, Silva DD, Coelho WS, Marinho-Carvalho MM, Sola-Penna M. 2011. Lactate downregulates the glycolytic enzymes hexokinase and phosphofructokinase in diverse tissues from mice. *FEBS Lett.* 585(1):92-98.
- Li J, Wong CL, Vijayasankaran N, Hudson T, Amanullah A. 2012. Feeding lactate for CHO cell culture processes: impact on culture metabolism and performance. *Biotechnol Bioeng.* 109(5):1173-1186.
- Lincet H, Icard P. 2015. How do glycolytic enzymes favour cancer cell proliferation by nonmetabolic functions? *Oncogene.* 34(29):3751-3759.
- Liste-Calleja L, Lecina M, Lopez-Repullo J, Albiol J, Solà C, Cairó JJ. 2015. Lactate and glucose concomitant consumption as a self-regulated pH detoxification mechanism in HEK293 cell cultures. *Appl Microbiol Biotechnol.* 99(23):9951-9960.
- López-Ríos F, Sánchez-Aragó M, García-García E, Ortega AD, Berrendero JR, Pozo-Rodríguez F, López-Encuentra A, Ballestín C, Cuezva JM. 2007. Loss of the mitochondrial bioenergetic capacity underlies the glucose avidity of carcinomas. *Cancer Res.* 67(19):9013-9017.
- Ma L, Tao Y, Duran A, Llado V, Galvez A, Barger JF, Castilla EA, Chen J, Yajima T, Porollo A. 2013. Control of nutrient stress-induced metabolic reprogramming by PKC ζ in tumorigenesis. *Cell.* 152(3):599-611.
- Marguerat S, Bähler J. 2012. Coordinating genome expression with cell size. *Trends Genet.* 28(11):560-565.
- Marshall WF, Young KD, Swaffer M, Wood E, Nurse P, Kimura A, Frankel J, Wallingford J, Walbot V, Qu X. 2012. What determines cell size? *BMC Biol.* 10(1):101.
- Martinez VS, Dietmair S, Quek L-E, Hodson MP, Gray P, Nielsen LK. 2013. Flux balance analysis of CHO cells before and after a metabolic switch from lactate production to consumption. *Biotechnol Bioeng.* 110(2):660-666.

- McVey D, Aronov M, Rizzi G, Cowan A, Scott C, Megill J, Russell R, Tirosh B. 2016. CHO cells knocked out for TSC2 display an improved productivity of antibodies under fed batch conditions. *Biotechnol Bioeng.* 113(9):1942-52.
- Merlo LMF, Pepper JW, Reid BJ, Maley CC. 2006. Cancer as an evolutionary and ecological process. *Nat Rev Cancer* 6(12):924-935.
- Metallo CM, Gameiro PA, Bell EL, Mattaini KR, Yang J, Hiller K, Jewell CM, Johnson ZR, Irvine DJ, Guarente L. 2012. Reductive glutamine metabolism by IDH1 mediates lipogenesis under hypoxia. *Nature* 481(7381):380-384.
- Miettinen TP, Pessa HK, Caldez MJ, Fuhrer T, Diril MK, Sauer U, Kaldis P, Björklund M. 2014. Identification of transcriptional and metabolic programs related to mammalian cell size. *Curr Biol.* 24(6):598-608.
- Mulukutla BC, Gramer M, Hu WS. 2012. On metabolic shift to lactate consumption in fed-batch culture of mammalian cells. *Metab Eng.* 14(2):138-149.
- O'Callaghan PM, Berthelot ME, Young RJ, Graham JW, Racher AJ, Aldana D. 2015. Diversity in host clone performance within a Chinese hamster ovary cell line. *Biotechnol Prog.* 31(5):1187-1200.
- Owens KM, Kulawiec M, Desouki MM, Vanniarajan A, Singh KK. 2011. Impaired OXPHOS complex III in breast cancer. *PloS one* 6(8):e23846.
- Pérez-Escuredo J, Dadhich RK, Dhup S, Cacace A, Van Hée VF, De Saedeleer CJ, Sboarina M, Rodriguez F, Fontenille M-J, Brisson L. 2016. Lactate promotes glutamine uptake and metabolism in oxidative cancer cells. *Cell Cycle* 15(1):72-83.
- Pires das Neves R, Jones NS, Andreu L, Gupta R, Enver T, Iborra FJ. 2010. Connecting variability in global transcription rate to mitochondrial variability. *PLoS Biol* 8(12):e1000560.
- Porter AJ. 2015. Three steps to start you on the path to obtaining the 'best' recombinant CHO cell line.
- Prentice HL, Ehrenfels BN, Sisk WP. 2007. Improving performance of mammalian cells in fed-batch processes through "bioreactor evolution". *Biotechnol Prog.* 23(2):458-464.
- Rodríguez-Enríquez S, Carreño-Fuentes L, Gallardo-Pérez JC, Saavedra E, Quezada H, Vega A, Marín-Hernández A, Olín-Sandoval V, Torres-Márquez ME, Moreno-Sánchez R. 2010. Oxidative phosphorylation is impaired by prolonged hypoxia in breast and possibly in cervix carcinoma. *Int J Biochem Cell Biol.* 42(10):1744-1751.
- Scarpulla RC. 2011. Metabolic control of mitochondrial biogenesis through the PGC-1 family regulatory network. *Biochim Biophys Acta.* 1813(7):1269-1278.

- Scarpulla RC, Vega RB, Kelly DP. 2012. Transcriptional integration of mitochondrial biogenesis. *Trends Endocrinol Metab.* 23(9):459-466.
- Schubert I, Vu GT. 2016. Genome stability and evolution: attempting a holistic view. *Trends Plant Sci.* 21(9):749-757.
- Scott DA, Richardson AD, Filipp FV, Knutzen CA, Chiang GG, Ze'ev AR, Osterman AL, Smith JW. 2011. Comparative metabolic flux profiling of melanoma cell lines: beyond the Warburg effect. *J Biol Chem.* 286(49):42626-42634.
- Sellick CA, Croxford AS, Maqsood AR, Stephens G, Westerhoff HV, Goodacre R, Dickson AJ. 2011. Metabolite profiling of recombinant CHO cells: designing tailored feeding regimes that enhance recombinant antibody production. *Biotechnol Bioeng.* 108(12):3025-3031.
- Sengupta N, Rose ST, Morgan JA. 2011. Metabolic Flux Analysis of CHO Cell Metabolism in the Late Non-Growth Phase. *Biotechnol Bioeng.* 108(1):82-92.
- Senyilmaz D, Teleman AA. 2015. Chicken or the egg: Warburg effect and mitochondrial dysfunction. *F1000prime reports* 7:41.
- Sinacore MS, Drapeau D, Adamson SR. 2000. Adaptation of mammalian cells to growth in serum-free media. *Mol Biotechnol.* 15(3):249-257.
- Smolková K, Plecítá-Hlavatá L, Bellance N, Benard G, Rossignol R, Ježek P. 2011. Waves of gene regulation suppress and then restore oxidative phosphorylation in cancer cells. *Int J Biochem Cell Biol.* 43(7):950-968.
- Son S, Tzur A, Weng Y, Jorgensen P, Kim J, Kirschner MW, Manalis SR. 2012. Direct observation of mammalian cell growth and size regulation. *Nat Methods.* 9(9):910-912.
- Sonveaux P, Végran F, Schroeder T, Wergin MC, Verrax J, Rabbani ZN, De Saedeleer CJ, Kennedy KM, Diepart C, Jordan BF. 2008. Targeting lactate-fueled respiration selectively kills hypoxic tumor cells in mice. *J Clin Invest.* 118(12):3930-3942.
- Stettler M, Jaccard N, Hacker D, Jesus MD, Wurm FM, Jordan M. 2006. New disposable tubes for rapid and precise biomass assessment for suspension cultures of mammalian cells. *Biotechnol Bioeng.* 95(6):1228-1233.
- Stopper H, Schmitt E, Gregor C, Mueller SO, Fischer WH. 2003. Increased cell proliferation is associated with genomic instability: elevated micronuclei frequencies in estradiol-treated human ovarian cancer cells. *Mutagenesis* 18(3):243-247.
- Swietach P, Vaughan-Jones RD, Harris AL, Hulikova A. 2014. The chemistry, physiology and pathology of pH in cancer. *Philos Trans R Soc Lond B Biol Sci.* 369(1638):20130099.

- Templeton N, Dean J, Reddy P, Young JD. 2013. Peak antibody production is associated with increased oxidative metabolism in an industrially relevant fed-batch CHO cell culture. *Biotechnol Bioeng.* 110(7):2013-24.
- TeSlaa T, Teitell MA. 2014. Techniques to monitor glycolysis. *Methods Enzymol.* 542:91.
- Tzur A, Kafri R, LeBleu VS, Lahav G, Kirschner MW. 2009. Cell growth and size homeostasis in proliferating animal cells. *Science* 325(5937):167-171.
- Vander Heiden MG, Cantley LC, Thompson CB. 2009. Understanding the Warburg effect: the metabolic requirements of cell proliferation. *Science* 324(5930):1029-33.
- Wallace DC. 2012. Mitochondria and cancer. *Nat Rev Cancer* 12(10):685-698.
- Warburg O. 1956. On the origin of cancer cells. *Science* 123(3191):309-314.
- Wilkins CA, Gerdtzen ZP. 2011. Engineering CHO cells for improved central carbon and energy metabolism. *BMC Proc.* 5(8):120.
- Wlaschin KF, Hu WS. 2007. Engineering cell metabolism for high-density cell culture via manipulation of sugar transport. *J Biotechnol. Netherlands.* p 168-76.
- Wong N, De Melo J, Tang D. 2013. PKM2, a central point of regulation in cancer metabolism. *Int J Cell Biol.* 2013:242513.
- Yang C, Sudderth J, Dang T, Bachoo RG, McDonald JG, DeBerardinis RJ. 2009. Glioblastoma cells require glutamate dehydrogenase to survive impairments of glucose metabolism or Akt signaling. *Cancer Res.* 69(20):7986-7993.
- Yang M, Vousden KH. 2016. Serine and one-carbon metabolism in cancer. *Nat Rev Cancer.* 16(10):650-62.
- Young JD. 2013. Metabolic flux rewiring in mammalian cell cultures. *Curr Opin Biotechnol.* 24(6):1108-1115.
- Zhang H, Gao P, Fukuda R, Kumar G, Krishnamachary B, Zeller KI, Dang CV, Semenza GL. 2007. HIF-1 inhibits mitochondrial biogenesis and cellular respiration in VHL-deficient renal cell carcinoma by repression of C-MYC activity. *Cancer cell* 11(5):407-420.
- Zheng J. 2012. Energy metabolism of cancer: Glycolysis versus oxidative phosphorylation (Review). *Oncol Lett.* 4(6):1151-1157.
- Zhou M, Crawford Y, Ng D, Tung J, Pynn AFJ, Meier A, Yuk IH, Vijayasankaran N, Leach K, Joly J and others. 2011. Decreasing lactate level and increasing antibody production in Chinese Hamster Ovary cells (CHO) by reducing the expression of lactate dehydrogenase and pyruvate dehydrogenase kinases. *J Biotechnol.* 153(1-2):27-34.

LIST OF FIGURES

Fig. 1. Cell specific growth rate performance for 22 clonally-derived CHO-S cell lines during long-term cell culture. Clonal populations were routinely cultivated in TubeSpin bioreactor tubes for up to 220 generations with a 3- to 4-day subculture regime. Cell samples were cryopreserved at 0, 80 and 200 generations representing adaptation, mid-evolution and maximally evolved phases, respectively. The inset illustrates the extent of growth variability in μ and the overall average rate of change in μ across the extended cultivation. The overall average rate of change in μ was calculated as the linear regression of the median values of the observed cell growth rates at every 40 generations. Statistical significance is indicated as follows * $P < 0.05$, ** $P < 0.01$, *** $P < 0.001$.

Fig. 2. FBC performance of the 22 clonal isolates across three stages of evolutionary subculture. Clonal isolates were removed from cryopreservation at 0, 80 and 200 generations, representing adaptation, mid-evolution and maximally evolved phases, respectively. Samples of the FBC flasks were taken daily for VCC (A) and IVCC (B) measurements until cell viability dropped below 60%. The cumulative IVCV during the first 7 days of culture (C) and post-day 7 (D) and IVCV at the end of FBC (F) of subclones.0 (dark grey bars), 80 (grey bars) and 200 (white bars) was calculated. The insets illustrate the extent of IVCCs accumulated to Day 7 (C) and post-Day 7 (D) across the three evolutionary phases. Plot E shows the negative correlation between average cell volume and μ (PPMCC $r = -0.56$; p -value < 0.001). The black, grey and white circles represent mid-evolution and maximally evolved phases, respectively. Statistical significance is indicated as follows * $P < 0.05$, ** $P < 0.01$, *** $P < 0.001$.

Fig. 3. FBC performance of selected clones across three stages of evolutionary subculture. FBC performance space (A) across 66 subclonal isolates at varying evolved stages. Cumulative

IVCV during the first 7 days of culture (B) and their subsequent cumulative IVCCs (C) of selected clones (as summarized in A) with low (dark grey bars), mid (grey bars) and high (white bars) FBC performance. The black, grey and white circles in A represent adaptation, mid-evolution and maximally evolved phases, respectively. The “X” represents the parental populations. Statistical significance is indicated as follows * P<0.05, ** P<0.01, *** P<0.001.

Fig. 4. Carbon flux metabolism of selected subclonal populations varying in FBC performance. Cell supernatants were sampled at mid-exponential and stationary growth phase for the measurement of glucose, lactate and glutamine. The figures show the specific glucose consumption rate (A), lactate net flux (B), and glutamine consumption rate (C), respectively. The dark grey, grey and white bars represent subclones with low, mid, and high FBC performance, respectively. The bottom and top of the box represent the 25th and 75th percentiles, the line within the box the median, error bars indicate the 0th and 100th percentiles and dots are outliers. Statistical significance is indicated as follows * P<0.05, ** P<0.01, *** P<0.001.

Fig. 5. Mitochondrial functions of selected subclonal populations varying in FBC performance. Cells were harvested at mid-exponential (Day 3; A) and stationary (Day 7; B) phase for the measurements of OCR. Triplicate measurements of the basal OCR were obtained in un-buffered DMEM, followed by triplicate measurements of OCR after injection of each of the following compounds: oligomycin, FCCP and rotenone/antimycin A. The basal mitochondrial respiration (C), ATP turnover (D), maximal respiration (E), spare respiratory capacity (F), proton leak (G), non-mitochondrial respiration (H), and coupling efficiency (I) at both growth phases was calculated. The dark grey, grey and white bars represent subclones with low, mid, and high FBC performance, respectively. The bottom and top of the box

represent the 25th and 75th percentiles, the line within the box the median, error bars indicate the 0th and 100th percentiles and dots are outliers. Statistical significance is indicated as follows * P<0.05, ** P<0.01, *** P<0.001.

Fig. 6. Glycolytic activity of selected subclonal populations varying in FBC performance.

Cells were harvested at mid-exponential (Day 3; A) and stationary (Day 7; B) phase for the measurements of their glycolytic activity. Triplicate measurements of basal ECAR were obtained in un-buffered DMEM, followed by triplicate measurements of ECAR after injection of each of the following compounds: glucose, oligomycin and 2-deoxy-glucose. The basal glycolytic acidification (C), glycolytic capacity (D), spare glycolytic capacity (E), and non-glycolytic acidification (F) at both growth phases was calculated. The dark grey, grey and white bars represent subclones with low, mid, and high FBC performance, respectively. The bottom and top of the box represent the 25th and 75th percentiles, the line within the box the median, error bars indicate the 0th and 100th percentiles and dots are outliers. Statistical significance is indicated as follows * P<0.05, ** P<0.01, *** P<0.001.

Fig. 7. High-performance cells exhibit increased recombinant protein production.

Five subpopulations with superior IVCC and IVCV performance and the parental host cell line were each transfected with 16.5 µg plasmid DNA encoding SEAP or Sp35Fc using Lipofectamine LTX with PLUS reagent. Samples of the transient FBC flasks were taken daily for VCC and cell size measurements until cell viability dropped below 60%. SEAP and Sp35Fc titers were measured at day 9 post-transfection. Comparisons of manufacturing performance in terms of titer (black bars), IVCC (grey bars), IVCV (striped bar) and cell specific production rate (white bars) at day 9 for SEAP and Sp35Fc are shown in (A) and (B), respectively. Data shown are the mean value ± standard deviation of two biological and two technical replicates.

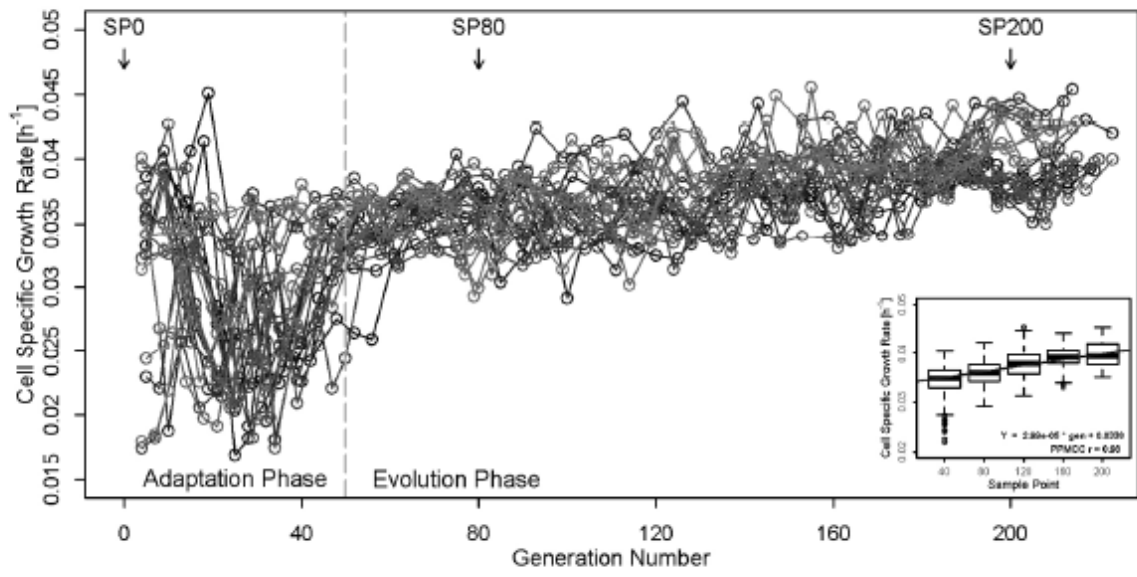


Figure 1

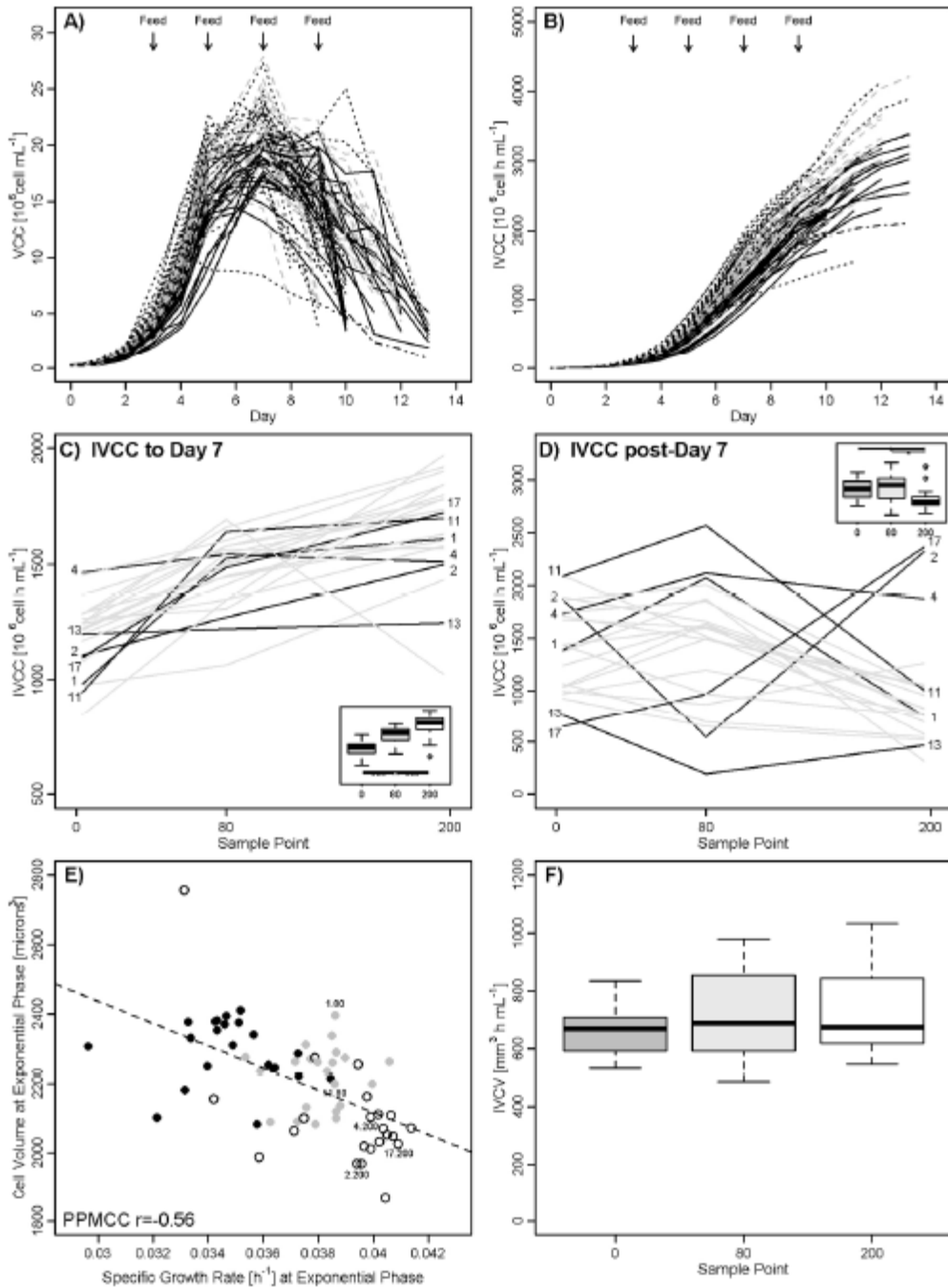


Figure 2

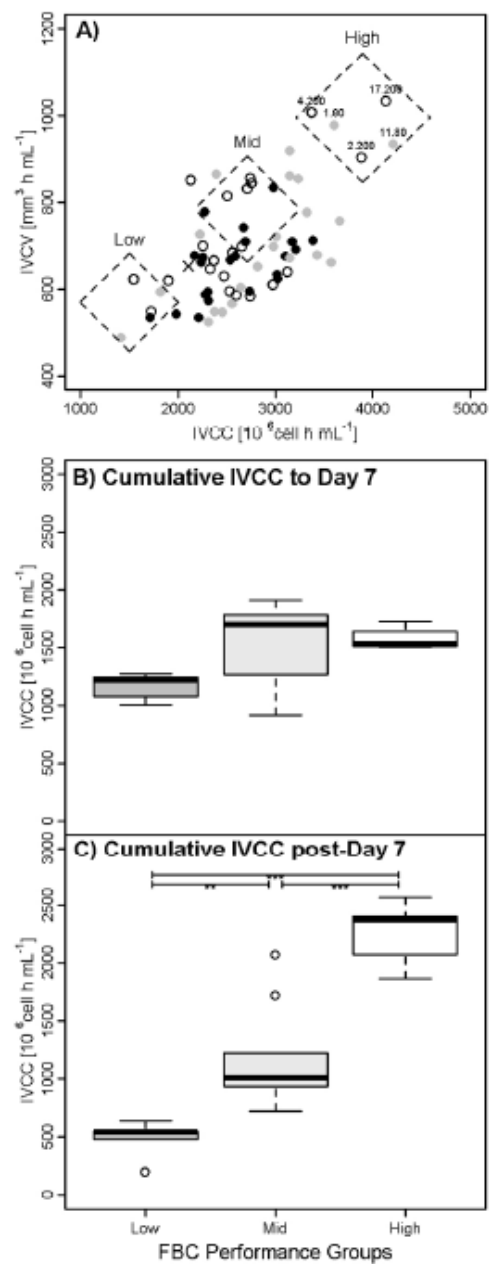


Figure 3

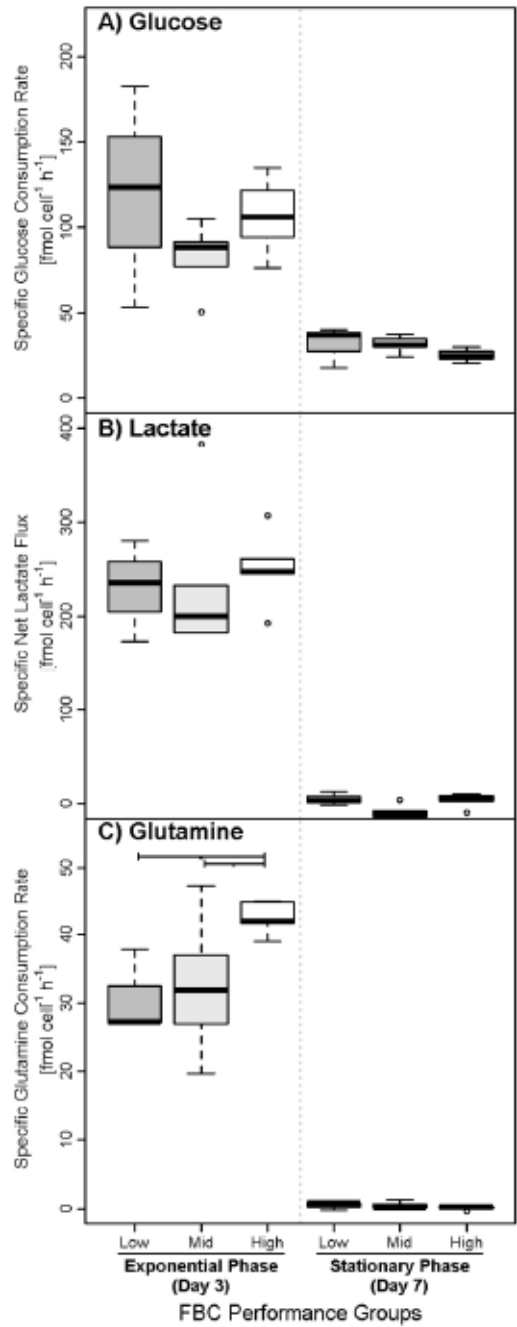


Figure 4

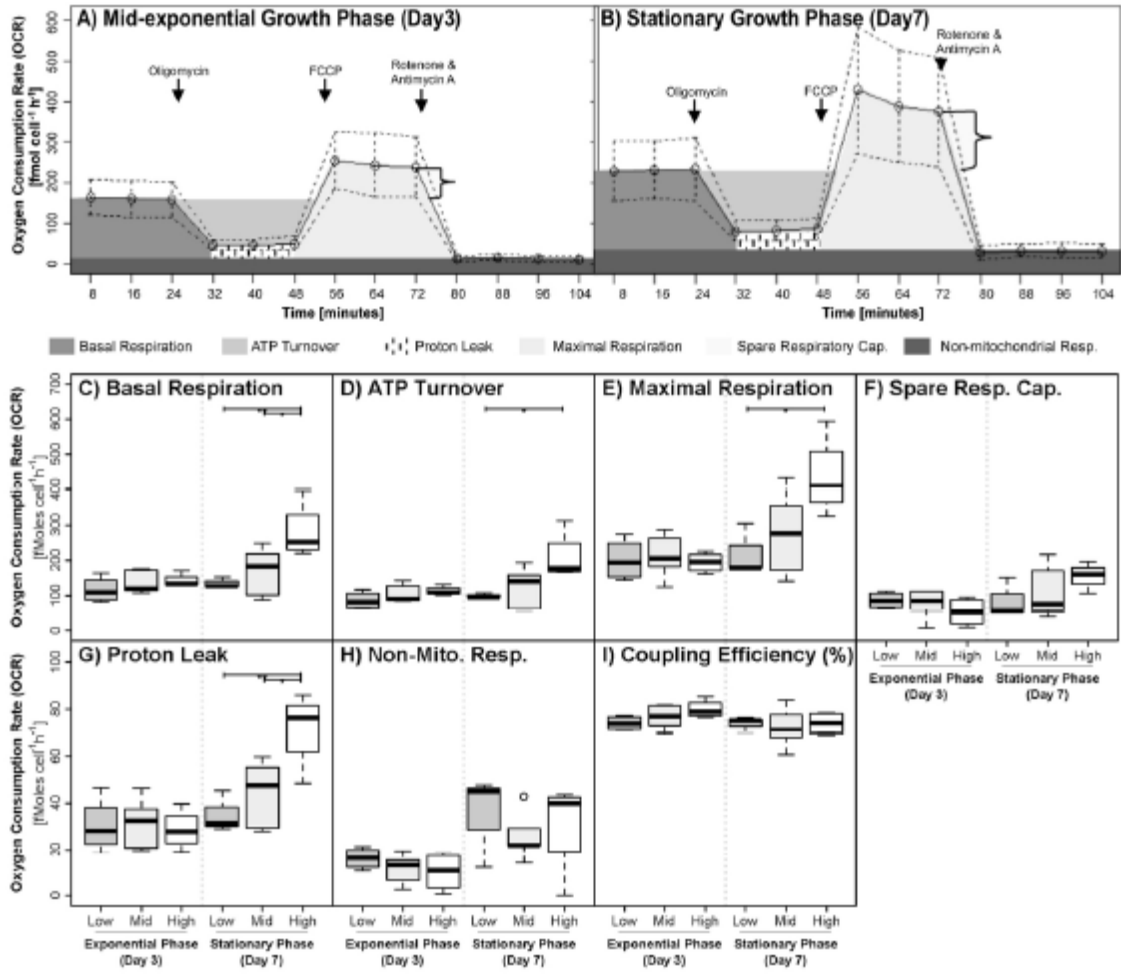


Figure 5

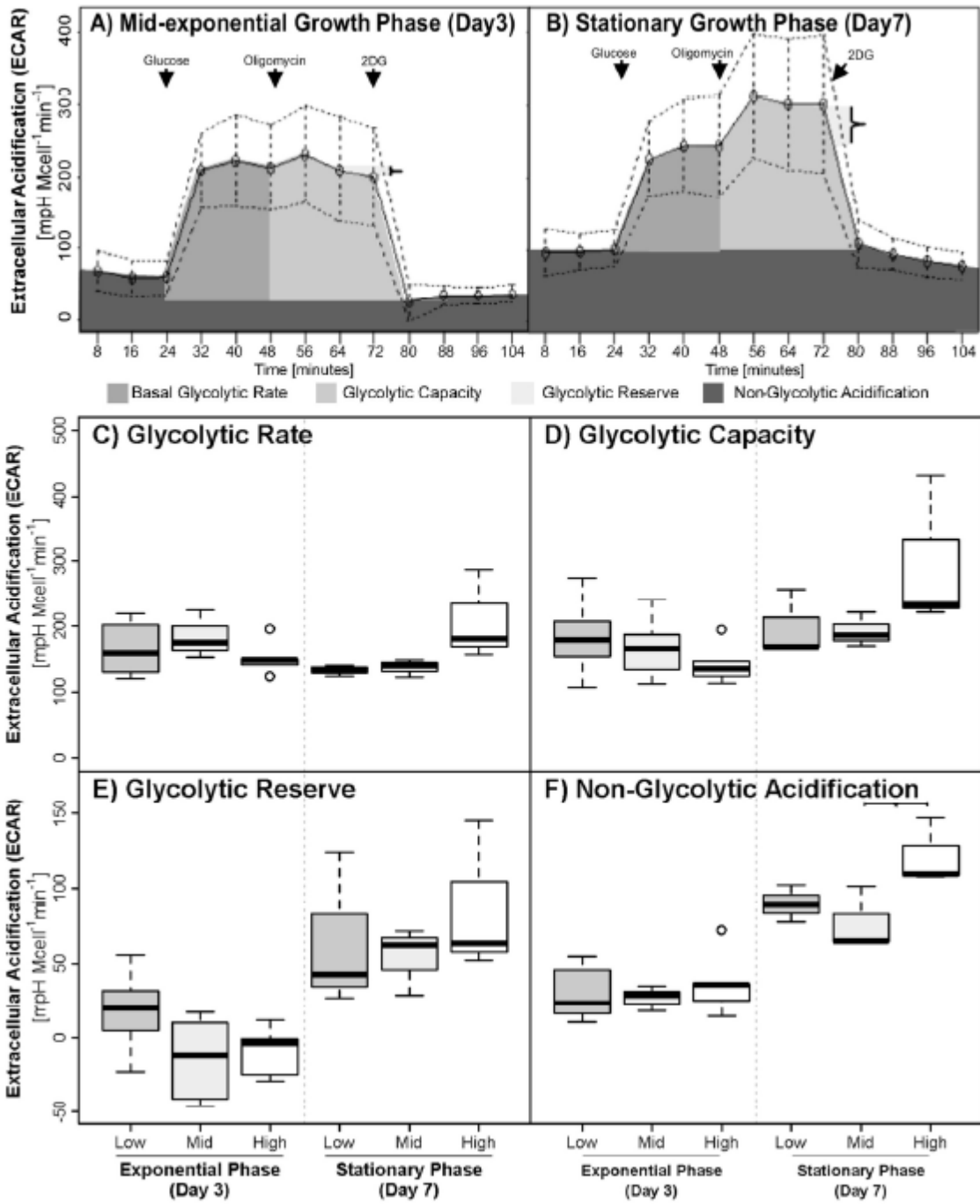


Figure 6

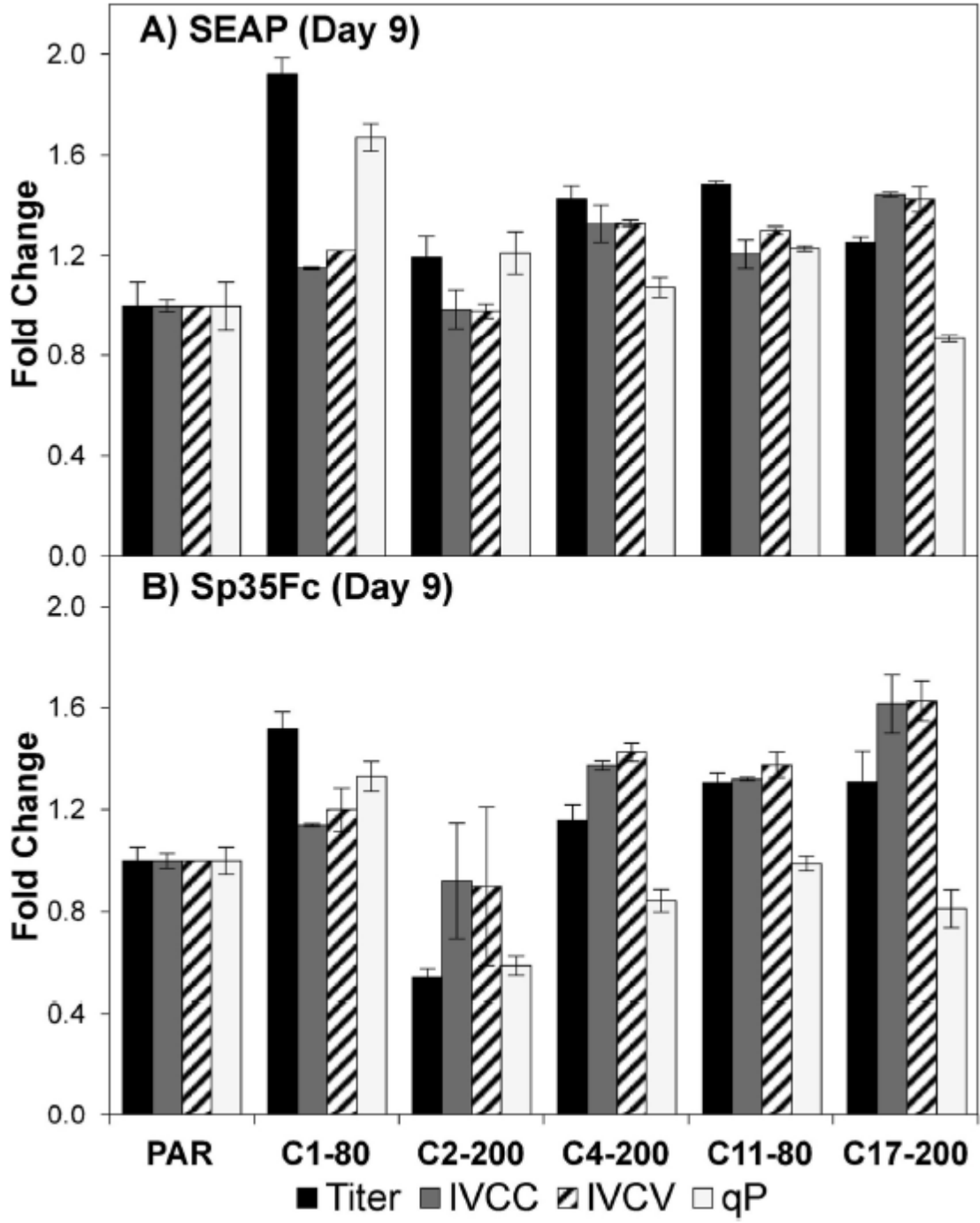


Figure 7